Large increases in N_{cn} and N_{ccn} together with a nucleation-mode-particle pool over the northwestern Pacific Ocean in the spring of 2014

Juntao Wang[1], Yanjie Shen[1], Kai Li[2], Yang Gao[1,3*], Huiwang Gao[1,3], Xiaohong Yao[1,3*]

[1]Key Lab of Marine Environmental Science and Ecology, Ministry of Education, Ocean University of China, Qingdao 266100, China
[2]National Marine Environmental Forecasting Center, Beijing, 100081, China
[3]Laboratory for Marine Ecology and Environmental Science, Qingdao National Laboratory for Marine Science and Technology, Qingdao 266071, China

Correspondence to: Yang Gao(Yanggao@ouc.edu.cn) and Xiaohong Yao (xhyao@ouc.edu.cn)

Abstract. The updated concentrations of atmospheric particles (N_{cn}) and the concentrations of cloud condensation nuclei (N_{ccn}) over the northwestern Pacific Ocean (NWPO) were important to accurately evaluate the influence of aerosol outflow from the Asian continent on the climate by considering rapid changes in emissions of air pollutants therein. However, field observations were scarce in the last two decades. We conducted a cruise campaign over the NWPO to simultaneously measure N_{cn}, N_{ccn} and the size distribution of aerosol particles from DOY 81 to DOY 108 of 2014. The mean values of N_{ccn} at supersaturation (SS) of 0.2% and 0.4% were $0.68 \pm 0.38 \times 10^3$ cm^{-3} and $1.1 \pm 0.67 \times 10^3$ cm^{-3}, respectively, with an average for N_{cn} of $2.8 \pm 1.0 \times 10^3$ cm^{-3} during the cruise over the NWPO, which were all approximately one order of magnitude larger than spring observations from two decades ago in the atmosphere of remote marine areas. The higher values, against the marine natural background reported in the literature, implied an overwhelming contribution from continental inputs. The calculated CCN activity ratios were 0.30 ± 0.11 and 0.46 ± 0.19 at SS of 0.2% and 0.4%, respectively, which were almost the same as those of upwind semi-urban sites. High N_{ccn} and CCN activities were observed from DOY 98 to 102, when the oceanic zone received even stronger continental inputs. During the whole cruise period with the exclusion of biomass burning and dust aerosols, a good correlation between N_{ccn} at 0.4% SS and the number concentrations of >60 nm particles ($N_{>60 nm}$), with the slope of 0.98 and $R^2=0.94$, was obtained, and the corresponding effective hygroscopicity parameter (κ) was estimated as 0.40. The bimodal size distribution pattern of the particle number concentration was generally observed during the entire campaign when the $N_{>90 nm}$ varied largely. However, the $N_{<30 nm}$, accounting for approximately 1/3 of the total number concentration, varied narrowly, and two NPF events associated with vertical transport were observed, implying a pool of nucleation mode atmospheric particles aloft. Biomass burning (BB) and dust events were observed over the NWPO, but the contributions of BB and dust aerosols to N_{cn} and N_{ccn} were minor (i.e., 10% or less) on the monthly time scale.

1 Introduction

In the atmosphere, aerosol particles (condensation nuclei, CN) being activated as cloud condensation nuclei (CCN) can indirectly affect the climate by altering clouds and precipitation (Yu and Luo, 2009; Yu et al., 2013). The role of marine atmospheric particles in the global climate system has attracted much attention, because the oceans cover nearly ~2/3 of the
5   Earth's surface, e.g., the CLAW hypothesis (Charlson et al., 1987; Quinn and Bates, 2011). In the atmosphere in marine areas, aerosol particles can be derived from a variety of sources, such as sea spray aerosols, long-range transport aerosols and the secondary aerosols formed via marine gaseous precursors or mixed marine and continent-derived gaseous precursors, etc. (Clark et al., 1998; Andreae and Rosenfeld, 2008; Feng et al., 2012; Liu et al., 2014; Guo et al., 2016; Feng et al., 2017). For example, ultrafine sea-salt aerosol particles released locally can be an important source of CCN in the marine atmosphere
10   (Clarke et al., 2006). Ocean-derived dimethylsulfide and other volatile organics can undergo photochemical reactions, and their oxidized products may nucleate into particles, which subsequently grow to be larger and act as CCN (Andreae and Rosenfeld, 2008; Hoffmann et al., 2016). The seasonal outflows of continental primary aerosols, such as dust particles and BB aerosols, can also influence N_{ccn} in the remote marine atmosphere (Nagao, 1999; Huebert, 2003). Chemical and physical properties of marine aerosols thereby reportedly had high variation because of dynamically varying contributions from these
15   primary sources and secondary formation pathways, leading to concentrations of CCN (N_{ccn}) and the CCN activity of aerosols that vastly depend on maritime locations and seasons (Clark et al., 1998; Roberts et al., 2006; Lana et al., 2012; Collins et al., 2013; Dunne et al., 2014).

The northwestern Pacific Ocean (NWPO) had reportedly received a large amount of continental anthropogenic air pollutants, biomass burning (BB) aerosols, natural dust and volcanic plumes, etc., in the winter and spring seasons, carried by
20   the East Asian Monsoon (Uematsu et al., 2004; Guo et al., 2016; Luo et al., 2016; Yu et al., 2016). The Kuroshio Extension leads the NWPO to be an active subtropical cyclone basins (Hu et al., 2018). Those oceanic cyclones reportedly enhanced primary production therein (Chang et al., 2017), and a potential influence on atmospheric chemistry is thereby expected due to the air/sea exchange (Quinn et al., 2015). Interactions between moisture and atmospheric aerosols have been proposed to deeply affect the climate (Deng et al., 2014; Wang et al., 2014). However, direct observational data of aerosol particles and
25   CCN in number concentrations remain limited in the remote atmosphere over the NWPO and the last spring observation can be traced back to 1996 (Nagao et al., 1999). On the other hand, dynamic changes in emissions of anthropogenic pollutants occurred on the Asian continent in the last two decades (Chan and Yao, 2008; Liu et al., 2013). Updated studies are thereby urgently needed to characterize atmospheric particles and activation of aerosol particles as CCN therein such as number concentrations of CN and CCN, particle number size distributions, particle sources, Kappa value and activation diameter, etc.
30   In this work, we measured the particle number size distributions, N_{ccn}, and other gaseous and particle pollutants in the marine atmosphere during a campaign from 18 March (day of year (DOY) 77) to 22 April (DOY 112) 2014 on an R/V (*Dong Fang Hong 2*) traveling from the marginal seas of China to the NWPO and back. We studied the spatiotemporal variability of the particle number concentration (N_{cn}) and particle number size distributions, as well as the N_{ccn} and CCN activities of aerosol

particles, with particular attention on measurements made on DOY 81 to DOY 108, when the R/V traveled in the NWPO. Several new findings have been revealed and discussed, e.g., large increases of N_{cn} and N_{ccn}, against historical data and many small contributions of dust and BB aerosols to N_{cn} and N_{ccn} on the monthly time scale, etc. This work may stimulate more studies that update the influence of the current outflow from the Asian continent on the climate.

2 Experimental design

2.1 Field observation

In this study, we made measurements of atmospheric particles during a cruise campaign on the R/V *Dong Fang Hong 2* over the NWPO during DOY 77- 112 in 2014 (Fig. 1). Atmospheric particles were sampled through conductive tubes (TSI, US) connected with a diffusion dryer filled with silica gel (TSI, US) and a splitter that split the air flow into different instruments. The total sampling line is approximately 1.5 m. The number size distributions of aerosol particles with mobility diameter ranging from 5.6 nm to 560 nm were measured using a high time resolution (one second) particle sizer, i.e., a Fast Mobility Particle Sizer (FMPS, TSI Model 3091), and the data obtained from the FMPS were corrected using the empirical correction procedure proposed by Zimmerman et al. (2015). Due to the malfunction of the Condensation Particle Counter (CPC) in the campaign, the coefficient of 1.25 was used to correct the total particle number concentration measured by the FMPS, and the coefficient was reasonably stable for side-by-side measurements between the FMPS and a CPC during several campaigns before and after. A continuous flow CCN counter (CCNC, DMT Model 100) was used to measure the bulk CCN concentration. The total flow rate of the CCNC was set to 0.45 L min^{-1}, with a sheath to sample flow ratio of 10. The CCNC was calibrated with ammonium sulfate particles following the procedure of Rose et al. (2008) before our observations. In this experiment, the N_{ccn} at five different supersaturation (SS) levels of 0.2%, 0.4%, 0.6%, 0.8% and 1.0% were measured. It took 5 minutes to collect the N_{ccn} at each SS, but the first one minute of data was discarded because of the establishment of supersaturation equilibrium. Completing a cycle from 0.2% of SS to 1.0% of SS required 28 minutes, including an additional 3 minutes from 1.0% of SS to 0.2% of SS to ensure a steady state. Those instruments were placed on the top floor lab of the vessel approximately 15 m above the sea surface.

In addition, a total of 19 total suspended particle (TSP) samples were collected during the campaign. The sampling duration varied from ~10 h to 22 h, depending on concentrations and anchoring times. The BB tracers were analyzed using a gas chromatography mass spectroscopy (GC-MS), and the detailed procedures of the analysis of the organic tracers were described by Feng et al. (2015). Moreover, sulfur dioxide (SO$_2$) was measured by a SO$_2$ Analyzer (Thermo Model 43i), nitrogen oxides (NO$_x$) were measured by a NO$_x$ Analyzer (Thermo Model 42i) and ozone (O$_3$) was measured by an O$_3$ Analyzer (Thermo Model 49i) in five-minute time resolution. Note that the measured mixing ratios of SO$_2$ and NO$_X$ during the cruise campaign apparently suffered from large analytic errors at 1-2 ppb levels and even below. The data were thereby used only for identifying the plumes from ship-self emissions, but not for characterizing background levels of SO$_2$ and NO$_x$ in the remote marine atmosphere.

2.2 Web-based data and on-site meteorological data

The 3-day air mass back trajectories were calculated using the Hybrid Single-Particle Lagrangian Integrated Trajectory (HYSPLIT) model from the NOAA Air Resources Laboratory to identify the origins of air masses. The 3-day backward trajectories starting at 1000 above mean sea level (a.m.s.l.) were performed every 4 hours. The fire spots that occurred in East Asia and the Siberian region were detected by the Fire Information for Resource Management System (FIRMS) using the Terra and Aqua satellites (http://firefly.geog.umd.edu/firemap). Meteorological data, including wind speed/direction, temperature, pressure and relative humidity, were simultaneously measured on board.

2.3 Data Screening

To study aerosol particles that were derived from local marine emissions and long-range transport from continents, we first carefully screened out the data suffering from ship self-emissions. We exhaustively removed the suspected data that conformed to the following: (1) particle number concentration increased dramatically in a short time accompanied by increased mixing ratios of pollutant gases; (2) the median mobility diameter of the dominant particle mode in those concentrated plumes was 22 ± 2 nm; and (3) wind speed was ≤1 m/s. This could lead to a few parts of non-ship self-emission signals being removed by mistake, but the remaining measurement signals can well represent the real concentrations of N_{cn} and N_{ccn} in the marine atmosphere. An example has been shown in Supporting Information (Fig. S1). After screening out ship self-emission signals, approximately 50% of the whole measurements are still available for data analysis.

3 Results and discussion

3.1 Spatiotemporal variation of N_{cn} and N_{ccn}

Fig. 2 shows the time series of minutely averaged N_{cn}, bulk N_{ccn} and CCN activity ratio (AR) at SS values of 0.2% and 0.4% during the measurement from DOY 77-112, 2014. A rapid decrease in N_{cn} was observed from the marginal seas of China to the NWPO, e.g., the N_{cn} of $5.2\pm2.4\times10^3$ cm^{-3} during the departure and return periods, including DOY 77-80 and DOY 109-112, respectively, against the N_{cn} of $2.8\pm1.0\times10^3$ cm^{-3} during the cruise over the NWPO on DOY 81-108 (Fig. 2b), with the lowest N_{cn} of $2.0\pm0.53\times10^3$ cm^{-3} during DOY 103-108. However, these values over the NWPO were approximately one order of magnitude larger than the values of <204 particle cm^{-3} representing typical remote marine aerosols in the western Pacific measured by Mochida et al. (2011) and <300 particle cm^{-3} reported by Ueda et al. (2016), which was less affected by industrial activity in the tropical Pacific and 248 particles cm^{-3} derived from marine air masses over the northeast Pacific reported by Hudson and Xie (1999). Quinn et al. (2017) reviewed a bunch of observations in marine atmospheres and proposed that the N_{cn} beyond 540 particles cm^{-3} were probably attributed to the substantial contribution from continental inputs. A long-term observation of the background marine aerosols in the Southern Ocean marine boundary layer supports this assumption (Gras and Keywood, 2017). Suppose that the value of 540 cm^{-3} represented the maximum contribution from marine natural sources,

the mean N_{cn} of 2.8×10^3 cm^{-3} over NWPO, during DOY 81-108, observed in this study indicated that at least 80% (on average) of N_{cn} was contributed by continental inputs. Even for the period of DOY 103-108 with the smallest N_{cn}, the percentage contribution from continental inputs using the same approach was still estimated to be as high as 73% on average, further implying the dominant contribution of continental inputs. Regarding the observed N_{cn} alone, the remote marine atmosphere over the NWPO have been polluted to some extent in the spring, and no traditionally defined clean marine atmosphere existed at that period.

The mean values of N_{ccn} during the departure and return periods were $1.7 \pm 1.0 \times 10^3$ and $3.3 \pm 2.0 \times 10^3$ at SS of 0.2% and 0.4% (SS of 0.2% and 0.4% represented the moderate and high values, respectively, in the remote marine atmosphere), respectively (Table S1). In contrast, the mean values of N_{ccn} at these two SS levels decreased by approximately 60%, with values of $0.68 \pm 0.38 \times 10^3$ cm^{-3} and $1.1 \pm 0.67 \times 10^3$ cm^{-3}, respectively, during the period from DOY 81-108. Considering the mean values of N_{ccn} and the availableness of N_{cn}, the N_{ccn} in the atmosphere over the NWPO can be divided into four periods, i.e., DOY 81-86 (Period 1, ending with no N_{cn} data because of instrument malfunction), DOY 87-97 April (Period 2, ending with a large increase in N_{ccn}), DOY 98-102 (Period 3, ending with a large decrease in N_{ccn} to the low value), and DOY 103-108 (Period 4), with relatively low values during Period 1, 2 and 4, and high values during Period 3 (Fig. 2a). For example, during Period 1, the mean N_{ccn} is $0.56 \pm 0.12 \times 10^3$ cm^{-3} at SS of 0.2% and $0.84 \pm 0.20 \times 10^3$ cm^{-3} at SS of 0.4%. In contrast, during Period 3, several spikes of N_{ccn} were observed, leading to increased values of $1.3 \pm 0.36 \times 10^3$ cm^{-3} at an SS of 0.2% and $2.2 \pm 0.72 \times 10^3$ cm^{-3} at SS of 0.4% (Table 1). As shown in Fig. 1, the R/V traveled a long distance across the remote oceanic zones, approximately 1000 km or more from the continent during Periods 1, 2 and 4; however, it was close to the Japan during Period 3, in which the continental transport may play a more important role in the number concentration.

The median daily N_{ccn} at SS of 0.2% were typically in the range of 15 to 30 cm^{-3} in summer over the Arctic because of the lack of anthropogenic aerosol contributions (Leck and Svensson, 2015). Hudson et al. (1998) reported the mean N_{ccn} at an SS of 0.2% was approximately 70 cm^{-3} over the summertime Southern Ocean, which could be representative of a clean maritime atmosphere. The even larger N_{ccn} ($0.68 \pm 0.38 \times 10^3$ cm^{-3}) measured over the NWPO in this study strongly indicated that the CCN was overwhelmingly derived from upwind continental inputs. The N_{ccn} at SS of 0.4% observed over the NWPO in this study was approximately one order of magnitude larger than the mean value of N_{ccn} at SS of 0.5% measured under the influence from the Asian continental air masses in the spring of 1994-1996 at Ogasawara Island (Nagao et al., 1999), implying a large increase in N_{ccn} over the NWPO in the last decades. However, the large N_{ccn} over NWPO was less than half of the values during the departure and return periods (i.e., $1.7 \pm 1.0 \times 10^3$ cm^{-3} with SS of 0.2% and $3.3 \pm 2.0 \times 10^3$ cm^{-3} with SS of 0.4%), comparable to the observed N_{ccn} in the spring of 2005 at Jeju Island, Korea (Kuwata et al., 2008). Both the higher N_{ccn} than NWPO during the departure/return period and at Jeju island (Kuwata et al., 2008) implied the possible large removal of atmospheric particles, which may enable activation as CCN during long-range transport (Guo et al., 2016).

3.2 Spatiotemporal variation of CCN activity and factor analysis

The AR was calculated as N_{ccn} at a certain SS divided by N_{cn} during the entire cruise period on DOY 81-108, 2014 over the NWPO (Fig. 2c). The values of 0.30±0.11 at SS of 0.2% and 0.46±0.19 at SS of 0.4% in this study were almost the same as those reported previously, i.e., 0.28 ±0.17 at SS=0.2% and 0.43 ±0.24 at SS=0.4% obtained in the spring of 2013 at an upwind semi-urban site in Qingdao, China (Li et al., 2015) and those obtained in other semi-urban atmospheres (Rose et al., 2010; Leng et al., 2014). In terms of the four periods, the values of AR slightly decreased to 0.21±0.06 at SS of 0.2% and 0.32±0.09 at SS of 0.4% during Period 1, similar to Period 2 and 4 (Table 1). The values during Period 3 increased to 0.38± 0.11 at SS of 0.2% and 0.64±0.18 at SS of 0.4%, close to those of 0.43±0.13 at SS of 0.2% and 0.61±0.15 at SS of 0.4% during a moderately heavy pollution event in the spring of 2013 in Qingdao (Li et al., 2015), implying the aerosol particles during Period 3 were aged to a high extent. We will return to this later.

Following those in the literature, the total number concentration ($N_{>D_p}$) of particles larger than a threshold diameter (D_p), can be used as a proxy for the N_{ccn}. As proposed by Dusek et al. (2006), aerosol particles with the size exceeding 60~70 nm could be activated as CCN at SS of 0.4%. In this study, $N_{>D_p}$ with D_p varying from 50 nm to 80 nm was calculated and a linear correlation was conducted with the values of N_{ccn} measured at SS of 0.4%. A good correlation was obtained between N_{ccn} and $N_{>60\ nm}$, with the slope of 0.98 and R^2=0.94 (Fig. 3). The corresponding effective hygroscopicity parameter (κ) was further estimated to be 0.40, close to the κ-value of continental atmospheric aerosols (~0.3) and smaller than that of marine atmospheric aerosols (~0.7) (Kreidenweis et al., 2009; Pöschl et al., 2009.; Rose et al., 2010). This was not surprising because of the overwhelming continental contribution to the N_{cn} measured over the NWPO in this study. Mochida et al (2010a) measured the κ-value around 0.50 ±0.05 at Okinawa Island, Japan, on 3-12 April 2008, implied a large contribution from ammonium sulfate aerosols. Iwamoto et al., (2016), however, reported the observational results at the tip of Noto Peninsula, Japan, on 3-29 October 2012 with the lower κ-value around 0.27 ±0.21 associated with a high proportion of organics in atmospheric particles.

The same test was conducted to establish the correlation between N_{ccn} at SS of 0.2% and $N_{>D_p}$. We obtained the best correlation between N_{ccn} and $N_{>92.5}$ nm, with R^2=0.92 and the slope of 1.40 (Fig. S2). The FMPS suffers from the weakness of a low size resolution in the size range of >100 nm, and no exact values of D_p and $N_{>D_p}$ corresponding to N_{ccn} at SS of 0.2% were further calculated.

The ratios of $N_{>60\ nm}/N_{ccn}$ were separately considered during the four periods, i.e., 1.06±0.43 and 1.04±0.24 at SS = 0.4% during Period 3 and 4, respectively (Fig. 4). Ammonium sulfate have the critical diameter (D_c) = 53 nm at SS=0.4% and was likely one of the major contributors of atmospheric particles larger than 60 nm during Periods 3 and 4. The standard deviation reflected its variation in relative contribution to some extent. The values of $N_{>60\ nm}/N_{ccn}$ increased to 1.30±0.36 and 1.64±0.62 at SS=0.4% during Period 1 and 2, respectively (Fig. 4). A few values of $N_{>60\ nm}/N_{ccn}$ beyond 1.5 corresponded to smaller values of N_{ccn}, i.e., $<2.5 \times 10^3$ cm^{-3}, implying that the aerosol particles were less hygroscopic. Part of the aerosols were either from biomass burning aerosols or dust aerosols, as discussed later.

3.3 Particle number size distributions and spatiotemporal variations in different sized particles

When the particle number size distributions were examined (Fig. 1), a trough was clearly identified in the particle size range of 50-90 nm during the entire campaign. The trough was conventionally referred to as the Hoppel effect associated with atmospheric particles be modified by nonprecipitating clouds (Hoppel et al., 1986, 1994a, 1994b). The in-cloud processing could lead atmospheric particles to be more aged and hygroscopic. The accumulation mode of atmospheric particles with diameters larger than 90 nm ($N_{>90\,nm}$) showed a clear decrease from $4.0\pm1.4\times10^3$ cm^{-3} on DOY 78 to $1.1\pm0.4\times10^3$ cm^{-3} on DOY 80 when the cruise is relatively far from the continent, and then oscillated around the lower value during Periods 1 and 2. The $N_{>90\,nm}$ evidently increased up to $2.3\pm0.6\times10^3$ cm^{-3} during Period 3 and then decreased to $1.1\pm1.1\times10^3$ cm^{-3} during Period 4. During the return trip, when approaching to the continent, the $N_{>90\,nm}$ increased up to $2.2\pm0.4\times10^3$ cm^{-3} on DOY 110 and $4.7\pm1.5\times10^3$ cm^{-3} on DOY 111 with the increasing contribution from continental input.

The nucleation mode particle concentrations in the size range of <30 nm ($N_{<30\,nm}$) generally dominated over the $N_{>90\,nm}$ in the atmosphere over the NWPO, but it was not the case during the departure and return periods and Period 3. Unlike $N_{>90\,nm}$, the $N_{<30\,nm}$ didn't show a clear decrease from the marginal seas to the NWPO, i.e., the values of $N_{<30\,nm}$ were $1.8\pm0.7\times10^3$ cm^{-3} on DOY 78 and $1.9\pm0.3\times10^3$ cm^{-3} on DOY 80. The $N_{<30\,nm}$ narrowly oscillated approximately $1.5\pm0.2\times10^3$ cm^{-3} during Period 1 and $1.4\pm0.1\times10^3$ cm^{-3} during Period 2. The $N_{<30\,nm}$ then decreased to $1.1\pm0.3\times10^3$ cm^{-3} during Period 3, although the corresponding $N_{>90\,nm}$ showed an evident increase as mentioned previously. The $N_{<30\,nm}$ were $1.0\pm1.0\times10^3$ cm^{-3} during Period 4. A strong continental input led to a sharp increase of $N_{<30\,nm}$ from $1.0\pm0.2\times10^3$ cm^{-3} on DOY 110 to $3.7\pm1.5\times10^3$ cm^{-3} on DOY 111. Note that the data suffering from ship self-emissions have been excluded exhaustively; thus, we hypothesize that the small decrease in $N_{<30\,nm}$ over the NWPO might be due to dynamic sources forming the nucleation mode particle pool along the track.

The Aitken mode, in the size range of 30-60 nm, can be clearly identified during the departure and return periods and Period 3, but the mode largely decreased and sometimes was undetectable during Periods 1, 2 and 4. There was no significant change in number concentrations of particles with diameters between 30-60 nm ($N_{30-60\,nm}$) from the marginal seas to the open ocean on DOY 78-80, i.e., $N_{30-60\,nm} = 1.9\pm0.6\times10^3$ cm^{-3} on DOY 78 and $1.7\pm0.2\times10^3$ cm^{-3} on DOY 80, which was similar to $N_{<30\,nm}$. However, $N_{30-60\,nm}$ then sharply decreased by approximately 40%, down to $1.1\pm0.2\times10^3$ cm^{-3} during Period 1 and $1.0\pm0.1\times10^3$ cm^{-3} during Period 2. The larger decrease in $N_{30-60\,nm}$ relative to $N_{<30\,nm}$ during the two periods could be due to either less nucleation mode particles being able to grow to Aitken mode particles or more Aitken mode particles being removed by the Hoppel effect. The $N_{30-60\,nm}$ of $1.0\pm0.4\times10^3$ cm^{-3} during Period 3 was almost the same as those during Periods 1 and 2, but the latter varied widely. The $N_{30-60\,nm}$ further decreased to $0.7\pm0.7\times10^3$ cm^{-3} during Period 4, but varied more widely, until the cruise returned and was close to the continent (i.e., value of $2.7\pm0.8\times10^3$ cm^{-3} on DOY 112). When the ratios of $N_{30-60\,nm}/N_{<30\,nm}$ were examined, the ratios were close to the unity on DOY 78-80. The ratios decreased afterwards and ranged from 0.6 to 0.8 during each Period, which may be explained by the two possibilities abovementioned.

During the autumn campaign over the western North Pacific in 2008, Mochida et al. (2011) reported that the number concentrations of atmospheric particles exhibited a bimodal distribution with peak diameter at an Aitken mode and an accumulation mode. During a winter campaign over the tropical and subtropical Pacific Oceans from 2011 to 2012, Ueda et al. (2016) also observed the bimodal distribution pattern of atmospheric particles in the number concentration, with peak diameters at 30-80 nm and 100-200 nm. In the south subtropical Pacific area (SSP), Ueda et al. (2016) observed nucleation mode atmospheric particles (<30 nm) occasionally. They attributed the nucleation mode particles to those generated from new particle formation events.

The overall particle size distribution was dominated by the nucleation mode during Periods 1, 2 and 4 but was dominated by the accumulation mode during Period 3 (Fig. 1). Considering the more important roles of accumulation mode particles, compared to nucleation mode, in modulating the CCN, the mean value of the associated AR during Period 3 therefore doubled that during Period 1, albeit the mean value of N_{cn} during Period 3 was only 25% higher than that of Period 1. Most of Aitken mode particles were likely unable to activate as CCN at SS≤ 0.4% (Dusek et al., 2006). Recently, Fan et al. (2018) reported that atmospheric particles smaller than 50 nm can be activated to form additional cloud droplets in a low-aerosol environment, where deep convective clouds can develop very high vapor supersaturation. In the NWPO, very high vapor supersaturation could also occur and might cause the Aitken mode particles to be activated into CCN. The hypothesis, however, needs more evidences to confirm.

3.4 New particle formation events in the NWPO

During the whole campaign over the NWPO, only two new particle formation (NPF) events were observed on DOY 98 and DOY 103. Unlike previous studies in the marginal seas of China (Liu et al., 2014; Meng et al., 2015) and in the south subtropical Pacific (Ueda et al., 2016), the events in this study lasted for a short time. The newly formed particles apparently grew to a size smaller than 20 nm during the events. The first NPF event was observed from 5:43 to 6:00 (UTC+8) on DOY 98 with the minimum diameter of particles at ~8 nm growing to ~14 nm (Fig. 5a). The averaged value of $N_{<30 nm}$ during the NPF event nearly doubled the value observed one hour before or after the NPF event, but the average value of $N_{30-100 nm}$ during the NPF event was almost unchanged (Fig. 5b). From 5:00 to 8:00 (UTC+8), the wind direction was almost constant and the wind speed narrowly varied (Fig. 5c). In terms of the second new particle event, the signal of newly formed particles intermittently observed for approximately one hour on DOY 103 (Fig. 5d).

In the literature, NPF events in remote marine atmospheres usually occurred aloft rather than in the lower layers of the marine boundary layer (MBL). Wiedensohler et al. (1996) and Buzorius et al. (2004) reported that ultrafine particles were produced above or in the upper layers of the MBL and mixed downward to the atmosphere above sea level. Clark et al. (1998) and McNaughton et al. (2004) also reported a nucleation event above the MBL during aircraft observations over the Pacific Ocean. Regarding the pool of nucleation mode particles in the atmosphere over the NWPO mentioned above, as well as only two NPF events observed for dozens of minutes, we can reasonably infer that NPF events very likely occurred frequently above or in the upper layers of the MBL. When the NPF occurred aloft, two scenarios could occur and lead to the unique

observations over the NWPO. In limited cases, where newly formed particles took a short time to be mixed down, the NPF events can then be detected in the lower layer of MBL. In the other scenario, the newly formed particles took a long time to be mixed down since they were originally formed above the MBL. In this scenario, no NPF event can be detected in the lower layer of the MBL with a time delay relative to that above the MBL. However, the preexisting new particles might lead to $N_{<30}$

5 nm in the atmosphere being much larger than the marine natural background and narrowly varying in the marine atmosphere over a large spatial scale. Based on the calculated air mass back trajectories over the NWPO at 500 m above the sea surface (not shown), air masses from above the MBL and even from the free troposphere can be mixed down to the lower layer of the MBL. However, the duration time varied greatly case by case.

3.5 The influence of wind speed on N_{ccn}

10 As was discussed in section 3.1, the major source of N_{ccn} is continental inputs. In addition, the wind speed may modulate the contribution of sea salt and vertical turbulence transport to the N_{ccn}. According to previous studies, a logarithmic relationship between wind speed and film drop sea salt is $\log N_{film} = 0.095U_{10} + 0.283$, where N_{film} is the number concentration (cm^{-3}) and U_{10} is the wind speed at 10 m above the sea surface (O'Dowd et al., 1993, 1997; de Leeuw et al., 2011). It is generally accepted that particle size larger than 0.05 μm can be activated as CCN in the marine atmospheric environment,

15 where SS of 0.2-0.3% was regularly reached. Under high wind speeds, sea salt aerosols could be important contributors to CCN in the MBL. For example, O'Dowd et al. (1997) reported that the sea-salt CCN concentration increased with the increase of wind speed, reaching 150 cm^{-3} at SS of 0.3% and a wind speed of 20 m/s.

To study the relationship between the N_{ccn} and the wind speeds, we plotted time series of the N_{ccn} at SS of 0.2%, wind speed and wind direction at ~10 m above the sea surface in the NWPO during the four periods of the cruise (Fig. 6). During

20 period 1, wind speeds varied from 0.9 m/s to 11.6 m/s, with a mean value of 6.7±2.8 m/s (Fig. 6a). The sea-salt CCN concentration at SS of 0.2% was reported as ~10 cm^{-3} at the wind speed of 10 m/s (O'Dowd et al., 1997), thereby accounting for less than 2% of N_{ccn} (0.56±0.12×10^3 cm^{-3} discussed in section 3.1). Wind speeds varied in a broad range of 0.8 m/s to 18.3 m/s, with a mean value of 8.3±3.7 m/s during Period 3 (Fig. 6c). Suppose that the value of 100 cm^{-3} at a wind speed of 20 m/s at SS of 0.2% represented the maximum contribution from sea-salt CCN (O'Dowd et al., 1997) , for Period 3 with the highest

25 N_{ccn} (1.3±0.36×10^3 cm^{-3} discussed in section 3.1), the contribution of sea-salt CCN accounted for less than 8%. The results implied a minor contribution to N_{ccn} from a sea salt contributor.

In terms of the vertical transport, Clarke et al. (2013) reported that CCN activated in MBL clouds were strongly influenced by entrainment from the free troposphere (FT). The common high-pressure system over the NWPO may promote the subsidence of CCN from the FT. In this study, N_{ccn} had no significant correlation with wind speed at 95% confidence when all

30 data were analyzed. Our results are consistent with previous studies, i.e., Ueda et al. (2016) reported that no positive correlation between number concentrations of <500 nm particles and wind speeds in the tropical and subtropical Pacific Ocean. However, an obvious correlation between N_{ccn} and wind speed was observed in a few short periods. For example, a positive correlation can be obtained during DOY 102 -103 (Fig. 6c), implicative of the fact that enhanced vertical transport of high N_{ccn} aloft was

likely attributable to increased wind speed, since a high wind speed generally diluted the air mass to some extent (Hudson and Xie, 1999). On the other hand, a negative correlation existed during DOY 92-94 (Fig. 6b). The phenomenon was argued as a low N_{ccn} aloft, possibly even lower than at the sea surface (Hudson et al., 1998; Hudson and Xie, 1999; Kim et al., 2014); therefore, the enhanced turbulence might lead cleaner air to be mixed down, resulting in the subsequent decreased N_{ccn}. We also found that N_{ccn} had no evident change with largely changed wind speed during a few periods, e.g., DOY 99-100 (Fig. 6c), possibly implying an even distribution in the vertical direction (Hudson et al., 1998).

3.6 Fingerprints and contributions of CN and CCN from BB and dust aerosols

The long-range transport of biomass burning and dust aerosols from the Asian continent to the NWPO has attracted much attention (Huebert, et al., 2003; Luo et al., 2016; Fu et al., 2018). For example, inorganic ions in TSP samples collected by Fu et al. (2018) on the same cruise of this study indicated that the remote NWPO could be influenced by biomass burning aerosols. Also on the same cruise reported by Luo et al. (2016), the occurrence of dust and dust mixed with anthropogenic pollutants could be observed over the NWPO. Thus, the contributions of the two sources to N_{cn} and N_{ccn} are examined below.

According to the 3-day back trajectories at 1000 m, most of the air masses were identified to originate from either Siberia or northeastern China during this cruise campaign (Fig. S3). In the spring of 2014, satellite data showed a large number of fire events occurring on these upwind continents (Fig. S4). A TSP sample was collected during the period from 11:10 on DOY 101 to 23:30 on DOY 102 (UTC+8), in which the mass concentration of levoglucosan (LEVO), a BB tracer, was as high as 65 ng m^{-3}. The value was one order of magnitude higher than those in the spring over the island of Chichi-jima from 2001 to 2004 (1.0 ng m^{-3}) and the island of Okinawa in 2009-2012 (3.09 ±3.70 ng m^{-3}) (Mochida et al., 2010b; Zhu et al., 2015). The time series of N_{cn}, the bulk N_{ccn}, N_{ccn}/N_{cn}, $N_{>60\,nm}/N_{ccn}$ and geometric median diameter of 100-334 nm particles (GMD$_{100-334}$) at SS of 0.4% during Period 3 (Fig. 7) indicated that the BB event occurred exactly during the period from 22:19 on DOY 101 to 3:49 on DOY 102 (UTC+8), belonging to the Period 3 (98-102) defined in this study. The averaged value of N_{cn} during these five and half hours (green shading in Fig. 7a) nearly doubled the mean value during all of Period 3. However, the averaged value of N_{ccn} was slightly smaller than the mean value of Period 3 (green shading in Fig. 7a). At SS=0.4%, the averaged value of N_{ccn}/N_{cn} decreased by 38% against the average value during the whole Period 3, whereas the averaged value of $N_{>60\,nm}/N_{ccn}$ was approximately 80% higher than that of Period 3 (green shading in Fig. 7b), suggesting that a large proportion of BB aerosol particles could not be activated as CCN. Due to the limited size cut of FMPS for submicron particles, only the range of the κ value can be roughly estimated with values <0.1. The κ values from the different BB aerosols were reported as 0.2±0.1 after a few hours of photochemical processing (Engelhart et al., 2012). Assuming that N_{cn} and N_{ccn} for these five and half hours (i.e., 22:19 on DOY 101 to 3:49 on DOY 102) were completely contributed by BB aerosols, the N_{cn} and N_{ccn} during the period accounted for 18% and 9%, respectively, relative to the corresponding total on DOY 101-102. We also found that the GMD$_{100-334}$ of the particles during the BB aerosol event reach a minimal value, decreased by ~10 nm relative to all of Period 3 (green shading in Fig. 7c). In addition to this sample collection from 22:19 on DOY 101 to 3:49 on DOY 102, the LEVO concentrations in other TSP samples were less than 13.7 ng m^{-3} with an average of 4.5 ng m^{-3}, indicating a large decrease in

loadings of BB aerosols, suggesting relatively smaller contributions of BB aerosols to N_{cn} and N_{ccn} during the other sampling periods.

During the period from 1:44 to 7:38 DOY 98 (UTC+8), the LiDAR browse from NASA (Fig. S5) detected the signal of dust sweeping over the measurement zone. The averaged value of N_{cn} during the dust event nearly doubled that of Period 3, with the averaged value of N_{ccn} decreasing by 27% (gray shading in Fig. 7a). Lee et al. (2009) modeled the influence of dust events on CCN and reported the maximum decrease of 20%. The averaged value of $N_{>60 nm}/N_{ccn}$ was computed as 2.3 and was even larger than that of BB aerosols (value of 1.8), and the estimated κ value of dust aerosols was smaller than 0.1. Although the uptake of sulfuric and nitric acids on dust aerosols may increase their hygroscopicity (Manktelow et al., 2010; Matsuki et al., 2010), apparently they had a negligible influence on their contribution to N_{ccn} at SS=0.4%. Additionally, assuming that N_{cn} and N_{ccn} from 1:44 to 7:38 on DOY 98 (UTC+8) were completely contributed by dust aerosols, the N_{cn} and N_{ccn} during these few hours accounted for 58% and 34%, respectively, relative to the corresponding totals of N_{cn} and N_{ccn} on DOY 98. In terms of the entire cruise period, if $N_{>60 nm}/N_{ccn}$ was greater than a certain threshold (i.e., 1.5, smaller than the value of 2.3 for $N_{>60 nm}/N_{ccn}$ during the dust event and the value of 1.8 for $N_{>60 nm}/N_{ccn}$ during the BB event), it was considered as the impact from dust and BB aerosols, and the subsequent summation of N_{ccn} and N_{cn} during these days over NWPO accounted for less than 10% of the total N_{ccn} and N_{cn} during this period, indicating a relatively minor contribution of dust and BB aerosols to N_{cn} and N_{ccn} on a monthly scale.

4 Conclusions

A field campaign to study the influence of the outflow from the Asian continent on the N_{cn}, N_{ccn} and number size distribution of aerosol particles over the NWPO was conducted during DOY 77-112. The average N_{cn} and N_{ccn} were approximately one order of magnitude higher than those observations previously reported in the remote marine atmosphere during other seasons or in the atmosphere of other remote marine areas, implying that the NWPO received more continental inputs due to the rapid increase in emissions of air pollutants in recent years during spring. The CCN activities were almost the same as those of the atmosphere of semi-urban areas, implicative of the aerosol particles over the NWPO being aged to some extent. The number concentration of accumulation mode atmospheric particles with diameters larger than 60 nm ($N_{>60 nm}$) had a good correlation with N_{ccn} at SS of 0.4%, with the $N_{>60 nm}/N_{ccn}$ ratio (0.98) close to 1. When we use D_p = 60 nm as a proxy for the D_c, the κ was estimated to be 0.40. The value slightly increased against the average value of 0.3 widely observed in upwind continental atmospheres, implying that additional aerosol aging during long-range transport in the marine atmosphere yielded a minor influence on *k*.

When the particle number size distribution was examined, a bimodal size distribution pattern was generally observed, and the particle size distribution was dominated by the nucleation mode in Period 1, while it was dominated by the accumulation mode in Period 3. The $N_{<30 nm}$ narrowly varied from the marginal sea to the NWPO, while the $N_{>90 nm}$ vastly changed in different periods, which implied that relatively stable sources generated the smaller size particles along the track. We found that

approximately 1/3 of N_{cn} was contributed from $N_{<30\ nm}$. Two NPF events were measured during the observation period. The vertical transport of newly formed particles to the lower layer of the MBL appeared to be important sources of nucleation mode particles measured along the track.

When the data measured during the entire campaign were used, no positive correlation between the N_{ccn} and wind speeds was obtained due to the minor contribution of the wind-driven particle production at the ocean surface. However, good positive or negative correlations between N_{ccn} and wind speed can be obtained in a few short periods. The possibly large gradient of N_{ccn} in the vertical direction together with enhanced or reduced vertical transport likely caused the correlations.

The intrusion events of BB and dust aerosols were occasionally observed over the NWPO. The N_{ccn} slightly decreased with increasing N_{cn} during dust and BB events. Combining the lower N_{ccn}/N_{cn} ratios and the higher $N_{>60\ nm}/N_{ccn}$ during those events, we speculated that a large proportion of particles are inactive to be activated to CCN. Meanwhile, we also found that a minor contribution of dust and BB aerosols to CN and CCN in the number concentration on the monthly time scale.

Acknowledgements

We would like to thank the support from the National Key Research and Development Program in China (No.2016YFC0200504) and the Natural Science Foundation of China (Grant No. 41576118).

Authors contribution

Juntao Wang, Yang Gao and Xiaohong Yao designed the project, processed the data and performed the analysis. Yanjie Shen, Kai Li, and Huiwang Gao were involved in planning and supervised the manuscript. Juntao Wang prepared the manuscript with contributions from all co-authors.

References

Andreae, M. O. and Rosenfeld, D.: Aerosol-cloud-precipitation interactions. Part 1. The nature and sources of cloud-active aerosols, Earth-Science Rev., 89(1–2), 13–41, doi:10.1016/j.earscirev.2008.03.001, 2008.

Buzorius, G., McNaughton, C. S., Clarke, A. D., Covert, D. S., Blomquist, B., Nielsen, K., and Brechtel, F. J.: Secondary aerosol formation in continental outflow conditions during ACE-Asia, J. Geophys. Res., 109, D24203, doi:10.1029/2004JD004749, 2004.

Chan, C. K. and Yao, X.: Air pollution in mega cities in China, Atmos. Environ., 42(1), 1–42, 2008.

Chang, Y. L., Miyazawa, Y., Oey, L. Y., Kodaira, T. and Huang, S.: The formation processes of phytoplankton growth and decline in mesoscale eddies in the western North Pacific Ocean, J. Geophys. Res. Ocean., 122(5), 4444–4455, doi:10.1002/2017JC012722, 2017.

Charlson, R. J., Lovelock, J. E., Andreae, M. O. and Warren, S. G.: Oceanic phytoplankton, atmospheric sulphur, cloud albedo and climate, Nature, 326(6114), 655-661, 1987.

Clark, A. D., Varner, J. L., Eisele, F., Mauldin, R. L., Tanner, D. and Litchy, M.: Particle production in the remote marine atmosphere : Cloud outflow and subsidence during ACE 1, J. Geophys. Res., 103(D13), 16397–16409, doi:10.1029/97JD02987, 1998.

Clarke, A. D., Owens, S. R. and Zhou, J.: An ultrafine sea-salt flux from breaking waves: Implications for cloud condensation nuclei in the remote marine atmosphere, J. Geophys. Res. Atmos., 111(D06202), 1–14, doi:10.1029/2005JD006565, 2006.

Clarke, A. D., Freitag, S., Simpson, R. M. C., Hudson, J. G., Howell, S. G., Brekhovskikh, V. L., Campos, T., Kapustin, V. N. and Zhou, J.: Free troposphere as a major source of CCN for the equatorial pacific boundary layer: Long-range transport and teleconnections, Atmos. Chem. Phys., 13(15), 7511–7529, doi:10.5194/acp-13-7511-2013, 2013.

Collins, D. B., Ault, A. P., Moffet, R. C., Ruppel, M. J., Cuadra-Rodriguez, L. A., Guasco, T. L., Corrigan, C. E., Pedler, B. E., Azam, F., Aluwihare, L. I., Bertram, T. H., Roberts, G. C., Grassian, V. H. and Prather, K. A.: Impact of marine biogeochemistry on the chemical mixing state and cloud forming ability of nascent sea spray aerosol, J. Geophys. Res. Atmos., 118(15), 8553–8565, doi:10.1002/jgrd.50598, 2013.

de Leeuw, G., Andreas, E. ., Anguelova, M. ., Fairall, C. W., Ernie, R., O'Dowd, C., Schulz, M. and Schwartz, S. E.: Production flux of seaspray aerosol, Rev. Geophys., 49(2010), 1–39, doi:10.1029/2010RG000349, 2011.

Deng, Y., Gao, T., Gao, H., Yao, X. and Xie, L.: Regional precipitation variability in East Asia related to climate and environmental factors during 1979-2012, Sci. Rep., 4, 1–13, doi:10.1038/srep05693, 2014.

Dunne, E. M., Mikkonen, S., Kokkola, H. and Korhonen, H.: A global process-based study of marine CCN trends and variability, Atmos. Chem. Phys., 14(24), 13631–13642, doi:10.5194/acp-14-13631-2014, 2014.

Dusek, U., Frank, G. P., Hildebrandt, L., Curtius, J., Schneider, J., Walter, S., Chand, D., Drewnick, F., Hings, S., Jung, D., Borrmann, S. and Andreae, M. O.: Size matters more than chemistry aerosol particles, Science, 312(5778), 1375–1378, doi:10.1126/science.1125261, 2006.

Engelhart, G. J., Hennigan, C. J., Miracolo, M. A., Robinson, A. L. and Pandis, S. N.: Cloud condensation nuclei activity of fresh primary and aged biomass burning aerosol, Atmos. Chem. Phys., 12(15), 7285–7293, doi:10.5194/acp-12-7285-2012, 2012.

Fan, J., Rosenfeld, D., Zhang, Y., Giangrande, S. E., Li, Z., Machado, L. A. T., Martin, S. T., Yang, Y., Wang, J., Artaxo, P., Barbosa, H. M. J., Braga, R. C., Comstock, J. M., Feng, Z., Gao, W., Gomes, H. B., Mei, F., Pöhlker, C., Pöhlker, M. L., Pöschl, U. and De Souza, R. A. F.: Substantial convection and precipitation enhancements by ultrafine aerosol particles, Science, 359(6374), 411–418, doi:10.1126/science.aan8461, 2018.

Feng, J., Guo, Z., Zhang, T., Yao, X., Chan, C. K. and Fang M.: Source and formation of secondary particulate matter in $PM_{2.5}$ in Asian continental outflow, J. Geophys. Res. Atmos., 117(D03302), 1–11, doi:10.1029/2011JD016400, 2012.

Feng, J., Hu, J., Xu, B., Hu, X., Sun, P., Han, W., Gu, Z., Yu, X. and Wu, M.: Characteristics and seasonal variation of organic matter in $PM_{2.5}$ at a regional background site of the Yangtze River Delta region, China, Atmos. Environ., 123, 288–297, 2015.

Feng, L., Shen, H., Zhu, Y., Gao, H. and Yao, X.: Insight into generation and evolution of sea-salt aerosols from field measurements in diversified marine and coastal atmospheres, Sci. Rep., 7, 1–12, doi:10.1038/srep41260, 2017.

Fu, J., Wang, B., Chen, Y. and Ma, Q.: The influence of continental air masses on the aerosols and nutrients deposition over the western North Pacific, Atmos. Environ., 172, 1–11, doi:10.1016/j.atmosenv.2017.10.041, 2018.

Gras, L. J. and Keywood, M.: Cloud condensation nuclei over the Southern Ocean: Wind dependence and seasonal cycles, Atmos. Chem. Phys., 17(7), 4419–4432, doi:10.5194/acp-17-4419-2017, 2017.

Guo, T., Li, K., Zhu, Y., Gao, H. and Yao, X.: Concentration and size distribution of particulate oxalate in marine and coastal atmospheres – Implication for the increased importance of oxalate in nanometer atmospheric particles, Atmos. Environ., 142, 19–31, 2016.

Hoffmann, E. H., Tilgner, A., Schrödner, R., Bräuer, P., Wolke, R. and Herrmann, H.: An advanced modeling study on the impacts and atmospheric implications of multiphase dimethyl sulfide chemistry, Proc. Natl. Acad. Sci., 113(42), 11776–11781, doi:10.1073/pnas.1606320113, 2016.

Hoppel, W. A., Frick, G. M. and Larson, R. E.: Effect of nonprecipitating clouds on the aerosol size distribution in the marine boundary layer, Geophys. Res. Lett., 13(2), 125–128, doi:10.1029/GL013i002p00125, 1986.

Hoppel, W. A., Frick, G. M., Fitzgerald, J. W. and Wattle, B. J.: A cloud chamber study of the effect that nonprecipitating water clouds have on the aerosol size distribution, Aerosol Sci. Technol., 20(1), 1-30, doi: 10.1080/02786829408959660, 1994a.

Hoppel, W. A., Frick, G. M., Fitzgerald, J. W. and Larson, R. E.: Marine boundary layer measurements of new particle formation and the effects nonprecipitating clouds have on aerosol size distribution, J. Geophys. Res., 99(D7), 14443, doi:10.1029/94JD00797, 1994b.

Hu, Q., Qu, K., Gao, H., Cui, C., Gao, Y. and Yao, X.: Large increases in primary trimethylaminium and secondary dimethylaminium in atmospheric particles associated with cyclonic eddies in the northwest Pacific Ocean, J. Geophys. Res., 123(D21), 12133-12146, doi:10.1029/2018JD028836, 2018.

Hudson, J. G., Xie, Y. and Yum, S. S.: Vertical distributions of cloud condensation nuclei spectra over the summertime Southern Ocean, J. Geophys. Res. Atmos., 103(D13), 16609–16624, doi:10.1029/97JD03438, 1998.

Hudson, J. G. and Xie, Y.: Vertical distributions of cloud condensation nuclei spectra over the summertime northeast Pacific and Atlantic Oceans, J. Geophys. Res., 104, 30219–30229, 1999.

Huebert, B. J.: An overview of ACE-Asia: Strategies for quantifying the relationships between Asian aerosols and their climatic impacts, J. Geophys. Res., 108(D23), 1-20, doi:10.1029/2003JD003550, 2003.

Iwamoto, Y., Kinouchi, K., Watanabe, K., Yamazaki, N. and Matsuki, A.: Simultaneous measurement of CCN Activity and chemical composition of fine-mode aerosols at Noto Peninsula, Japan, in autumn 2012, Aerosol Air Qual. Res., 16, 2107-2118, doi:10.4209/aaqr.2015.09.0545, 2016.

Kim, J. H., Yum, S. S., Shim, S., Kim, W. J., Park, M., Kim, J. H., Kim, M. H. and Yoon, S. C.: On the submicron aerosol distributions and CCN number concentrations in and around the Korean Peninsula, Atmos. Chem. Phys., 14(16), 8763–8779, doi:10.5194/acp-14-8763-2014, 2014.

Kreidenweis, S. M., Petters, M. D. and Chuang, P. Y.: From the Strüngmann Forum Report, Clouds in the Perturbed Climate System: Their Relationship to Energy Balance, Atmospheric Dynamics, and Precipitation. Part 13: Cloud Particle Precursors. Edited by Jost Heintzenberg and Robert J. Charlson, MIT Press, Cambridge, 291-317, 2009.

Kuwata, M., Kondo, Y., Miyazaki, Y., Komazaki, Y., Kim, J. H., Yum, S. S., Tanimoto, H. and Matsueda, H.: Cloud condensation nuclei activity at Jeju Island, Korea in spring 2005, Atmos. Chem. Phys., 8(11), 2933–2948, doi:10.5194/acp-8-2933-2008, 2008.

Lana, A., Simó, R., Vallina, S. M. and Dachs, J.: Potential for a biogenic influence on cloud microphysics over the ocean: A correlation study with satellite-derived data, Atmos. Chem. Phys., 12(17), 7977–7993, doi:10.5194/acp-12-7977-2012, 2012.

Leck, C. and Svensson, E.: Importance of aerosol composition and mixing state for cloud droplet activation over the Arctic pack ice in summer, Atmos. Chem. Phys., 15(5), 2545–2568, doi:10.5194/acp-15-2545-2015, 2015.

Lee, Y. H., Chen, K. and Adams, P. J.: Development of a global model of mineral dust aerosol microphysics, Atmos. Chem. Phys., 9(7), 2441–2458, doi:10.5194/acp-9-2441-2009, 2009.

Leng, C., Zhang, Q., Zhang, D., Xu, C., Cheng, T., Zhang, R., Tao, J., Chen, J., Zha, S., Zhang, Y., Li, X., Kong, L. and Gao, W.: Variations of cloud condensation nuclei (CCN) and aerosol activity during fog-haze episode: A case study from Shanghai, Atmos. Chem. Phys., 14(22), 12499–12512, doi:10.5194/acp-14-12499-2014, 2014.

Li, K., Zhu, Y., Gao, H. and Yao, X.: A comparative study of cloud condensation nuclei measured between non-heating and heating periods at a suburb site of Qingdao in the North China, Atmos. Environ., 112, 40–53, 2015.

Liu, X., Zhang, Y., Han, W., Tang, A., Shen, J., Cui, Z., Vitousek, P., Erisman, J. W., Goulding, K., Christie, P., Fangmeier, A. and Zhang, F.: Enhanced nitrogen deposition over China, Nature, 494(7438), 459–462, doi:10.1038/nature11917, 2013.

Liu, X. H., Zhu, Y. J., Zheng, M., Gao, H. W. and Yao, X. H.: Production and growth of new particles during two cruise campaigns in the marginal seas of China, Atmos. Chem. Phys., 14(15), 7941–7951, doi:10.5194/acp-14-7941-2014, 2014.

Luo, L., Yao, X. H., Gao, H. W., Hsu, S. C., Li, J. W. and Kao, S. J.: Nitrogen speciation in various types of aerosols in spring over the northwestern Pacific Ocean, Atmos. Chem. Phys., 16(1), 325–341, doi:10.5194/acp-16-325-2016, 2016.

Manktelow, P. T., Carslaw, K. S., Mann, G. W. and Spracklen, D. V.: The impact of dust on sulfate aerosol, CN and CCN during an East Asian dust storm, Atmos. Chem. Phys., 10(2), 365–382, doi:10.5194/acp-10-365-2010, 2010.

Matsuki, A., Schwarzenboeck, A., Venzac, H., Laj, P., Crumeyrolle, S. and Gomes, L.: Cloud processing of mineral dust: Direct comparison of cloud residual and clear sky particles during AMMA aircraft campaign in summer 2006, Atmos. Chem. Phys., 10(3), 1057–1069, doi:10.5194/acp-10-1057-2010, 2010.

McNaughton, C. S., Clarke, A. D., Howell, S. G., Moore, K. G., Brekhovskikh, V., Weber, R. J., Orsini, D. A., Covert, D. S.,
5   Buzorius, G., Brechtel, F. J., Carmichael, G. R., Tang, Y., Eisele, F. L., Mauldin, R. L., Bandy, A. R., Thornton, D. C. and Blomquist, B.: Spatial distribution and size evolution of particles in Asian outflow: Significance of primary and secondary aerosols during ACE-Asia and TRACE-P, J. Geophys. Res. D Atmos., 109(19), 1–19, doi:10.1029/2003JD003528, 2004.

Meng, H., Zhu, Y., Evans, G. J. and Yao, X.: An approach to investigate new particle formation in the vertical direction on the
10   basis of high time-resolution measurements at ground level and sea level, Atmos. Environ., 102, 366–375, doi:10.1016/j.atmosenv.2014.12.016, 2015.

Mochida, M., Nishita-Hara, C., Kitamori, Y., Aggarwal, S. G., Kawamura, K. Miura, K. and Takami, A.: Size‐segregated measurements of cloud condensation nucleus activity and hygroscopic growth for aerosols at Cape Hedo, Japan, in spring 2008, J. Geophys. Res. Atmos., 115(D21207), 1–16, doi: 10.1029/2009JD013216, 2010a.

15   Mochida, M., Kawamura, K., Fu, P. and Takemura, T.: Seasonal variation of levoglucosan in aerosols over the western North Pacific and its assessment as a biomass-burning tracer, Atmos. Environ., 44(29), 3511–3518, doi:10.1016/j.atmosenv.2010.06.017, 2010b.

Mochida, M., Nishita-Hara, C., Furutani, H., Miyazaki, Y., Jung, J., Kawamura, K. and Uematsu, M.: Hygroscopicity and cloud condensation nucleus activity of marine aerosol particles over the western North Pacific, J. Geophys. Res. Atmos.,
20   116(6), 1–16, doi:10.1029/2010JD014759, 2011.

Nagao, I., Matsumoto, K., Tanaka, H.: Characteristics of dimethylsulfide, ozone, aerosols, and cloud condensation nuclei in air masses over the northwestern Pacific Ocean, J. Geophys. Res., 104(D9), 11675–11693, 1999.

O'Dowd, C. D., Smith, M. H. and Jennings, S. G.: Physico-chemical properties of aerosol over the Northeast Atlantic: Evidence for wind speed related submicron sea salt production, J. Geophys. Res., 98, 1137–1149, 1993.

25   O'Dowd, C. D., Smith, M. H., Consterdine, I. E. and Lowe, J. A.: Marine aerosol, sea-salt, and the marine sulphur cycle: A short review, Atmos. Environ., 31(1), 73–80, doi:10.1016/S1352-2310(96)00106-9, 1997.

Pöschl, U., Rose, D. and Andreae, M. O.: Climatologies of Cloudrelated Aerosols. Part 2: Particle Hygroscopicity and Cloud Condensation Nuclei Activity. In: Heintzenberg, J. and Charlson, R.J., Eds., Clouds in the Perturbed Climate System: Their Relationship to Energy Balance, Atmospheric Dynamics, and Precipitation, MIT Press, Cambridge, 58-72, 2009.

30   Quinn, P. K. and Bates, T. S.: The case against climate regulation via oceanic phytoplankton sulphur emissions, Nature, 480(7375), 51–56, doi:10.1038/nature10580, 2011.

Quinn, P. K., Collins, D. B., Grassian, V. H., Prather, K. A. and Bates, T. S.: Chemistry and related properties of freshly emitted sea spray aerosol, Chem. Rev., 115(10), 4383–4399, doi:10.1021/cr500713g, 2015.

Quinn, P. K., Coffman, D. J., Johnson, J. E., Upchurch, L. M. and Bates, T. S.: Small fraction of marine cloud condensation nuclei made up of sea spray aerosol, Nat. Geosci., 10(9), 674–679, doi:10.1038/ngeo3003, 2017.

Roberts, G., Mauger, G., Hadley, O. and Ramanathan, V.: North American and Asian aerosols over the eastern Pacific Ocean and their role in regulating cloud condensation nuclei, J. Geophys. Res., 111(D13205), 1-14, doi:10.1029/2005JD006661, 2006.

Rose, D., Gunthe, S. S., Mikhailov, E., Frank, G. P., Dusek, U., Andreae, M. O. and Pöschl, U.: Calibration and measurement uncertainties of a continuous-flow cloud condensation nuclei counter (DMT-CCNC): CCN activation of ammonium sulfate and sodium chloride aerosol particles in theory and experiment, Atmos. Chem. Phys., 8(5), 1153–1179, doi:10.5194/acp-8-1153-2008, 2008.

Rose, D., Nowak, A., Achtert, P., Wiedensohler, A., Hu, M., Shao, M., Zhang, Y., Andreae, M. O. and Pöschl, U.: Cloud condensation nuclei in polluted air and biomass burning smoke near the mega-city Guangzhou, China - Part 1: Size-resolved measurements and implications for the modeling of aerosol particle hygroscopicity and CCN activity, Atmos. Chem. Phys., 10(7), 3365–3383, doi:10.5194/acp-10-3365-2010, 2010.

Ueda, S., Miura, K., Kawata, R., Furutani, H., Uematsu, M., Omori, Y. and Tanimoto, H.: Number−size distribution of aerosol particles and new particle formation events in tropical and subtropical Pacific Oceans, Atmos. Environ., 142, 324–339, doi:10.1016/j.atmosenv.2016.07.055, 2016.

Uematsu, M., Toratani, M., Kajino, M., Narita, Y., Senga, Y. and Kimoto, T.: Enhancement of primary productivity in the western North Pacific caused by the eruption of the Miyake-jima Volcano, Geophys. Res. Lett., 31(6), 1–4, doi:10.1029/2003GL018790, 2004.

Wang, Y., Zhang, R. and Saravanan, R.: Asian pollution climatically modulates mid-latitude cyclones following hierarchical modelling and observational analysis, Nat. Commun., 5, 1–7, doi:10.1038/ncomms4098, 2014.

Wiedensohler, A., Covert, D. S., Swietlicki, E., Aalto, P., Heintzenberg, J. and Leck, C.: Occurrence of an ultrafine particle mode less than 20 nm in diameter in the marine boundary layer during Arctic summer and autumn, Tellus, 48(2), 213–222, doi:10.3402/tellusb.v48i2.15887, 1996.

Yu, F. and Luo, G.: Simulation of particle size distribution with a global aerosol model: contribution of nucleation to aerosol and CCN number concentrations, Atmos. Chem. Phys., 9(20), 7691–7710, doi:10.5194/acp-9-7691-2009, 2009.

Yu, F., Ma, X. and Luo, G.: Anthropogenic contribution to cloud condensation nuclei and the first aerosol indirect climate effect, Environ. Res. Lett., 8(2), 1-8,doi:10.1088/1748-9326/8/2/024029, 2013.

Yu, P., Hu, Q., Li, K., Zhu, Y., Liu, X., Gao, H. and Yao, X.: Characteristics of dimethylaminium and trimethylaminium in atmospheric particles ranging from supermicron to nanometer sizes over eutrophic marginal seas of China and oligotrophic open oceans, Sci. Total Environ., 572, 813–824, doi:10.1016/j.scitotenv.2016.07.114, 2016.

Zhu, C., Kawamura, K. and Kunwar, B.: Effect of biomass burning over the western North Pacific Rim: Wintertime maxima of anhydrosugars in ambient aerosols from Okinawa, Atmos. Chem. Phys., 15(4), 1959–1973, doi:10.5194/acp-15-1959-2015, 2015.

Zimmerman, N., Jeong, C. H., Wang, J. M., Ramos, M., Wallace, J. S. and Evans, G. J.: A source-independent empirical correction procedure for the fast mobility and engine exhaust particle sizers, Atmos. Environ., 100, 178–184, doi:10.1016/j.atmosenv.2014.10.054, 2015.
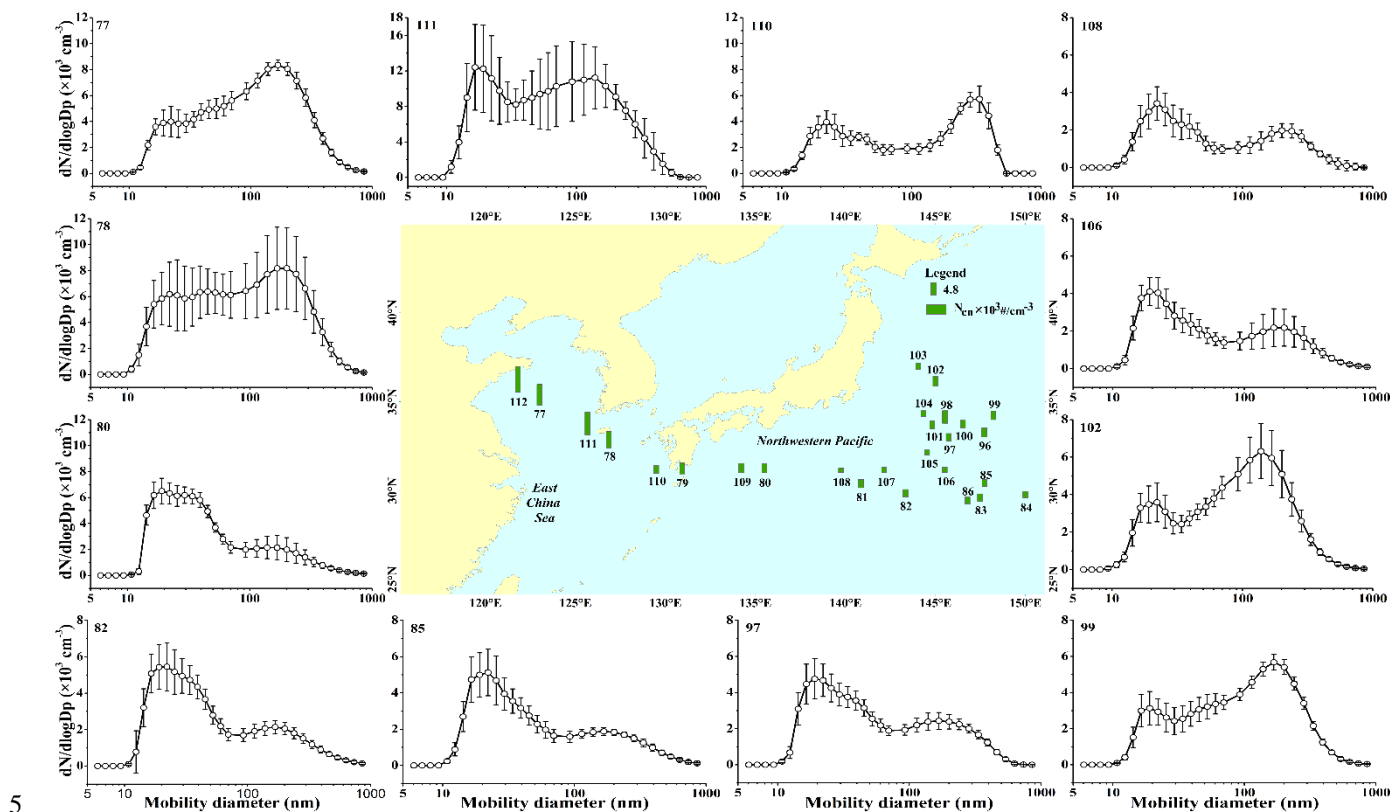
Figure 1 Geographical distributions of daily N_{cn} and number-size distribution of aerosol particles measured over the NWPO during DOY 77-112, 2014. The entire cruise was divided into five periods, including departure and return periods (77-80,109-112), Period 1(81-86), Period 2 (87-97), Period 3 (98-102) and Period 4 (103-108). For each period, the mode distribution is relatively comparable; thus, only a few days were selected to show the number size distributions, with the cruise day showing on the top left, corresponding to the number in the middle map.
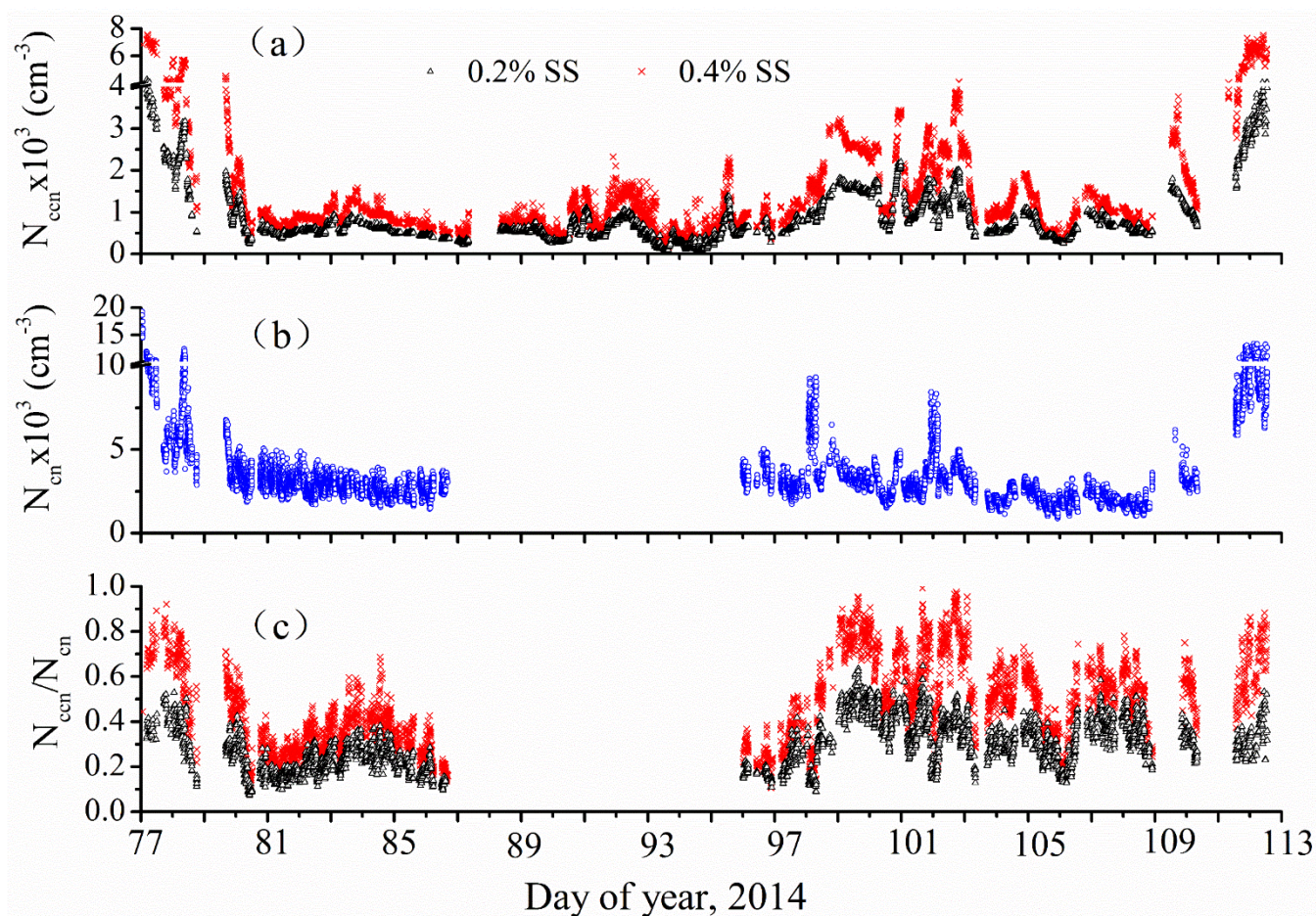
Figure 2 Time series of minutely averaged N_{cn}, bulk N_{ccn} and N_{ccn}/N_{cn} at SS of 0.2% and 0.4% during DOY 77-112, 2014.
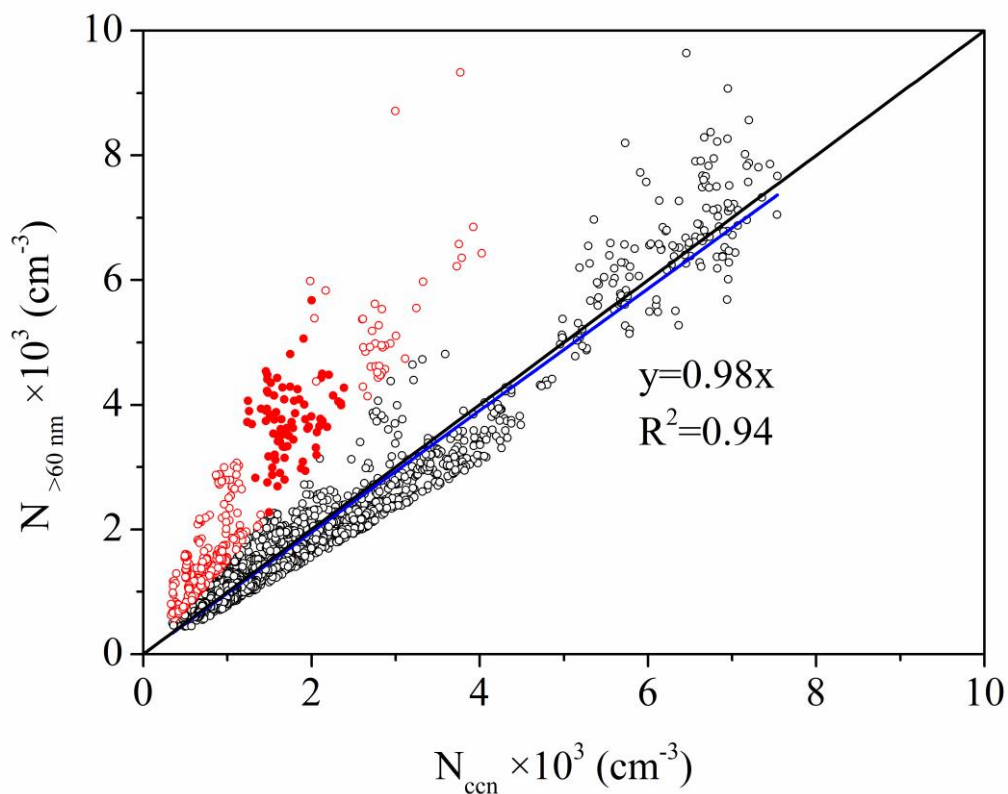
Figure 3 Scatterplots of N_{ccn} at SS of 0.4% versus $N_{>60 nm}$. (BB and dust aerosols are shown in full red cycles with empty red cycles representing suspected either BB or dust aerosols; the black line represents the 1:1 relationship, and the blue line shows the best fit using the data shown as black empty cycles.)
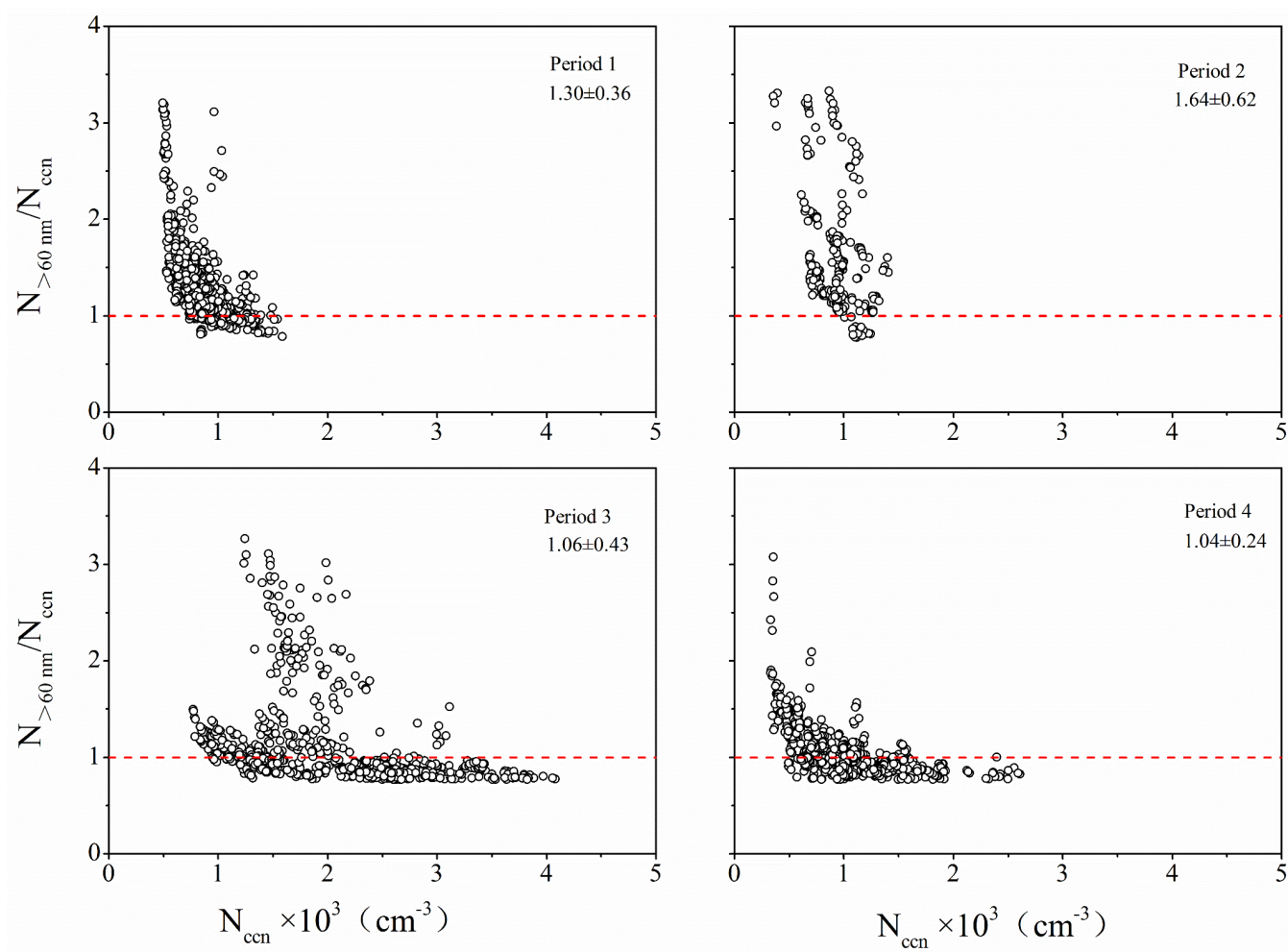
Figure 4 The ratios of $N_{>60\,nm}/N_{ccn}$ as a function of N_{ccn} at SS of 0.4% in different periods.
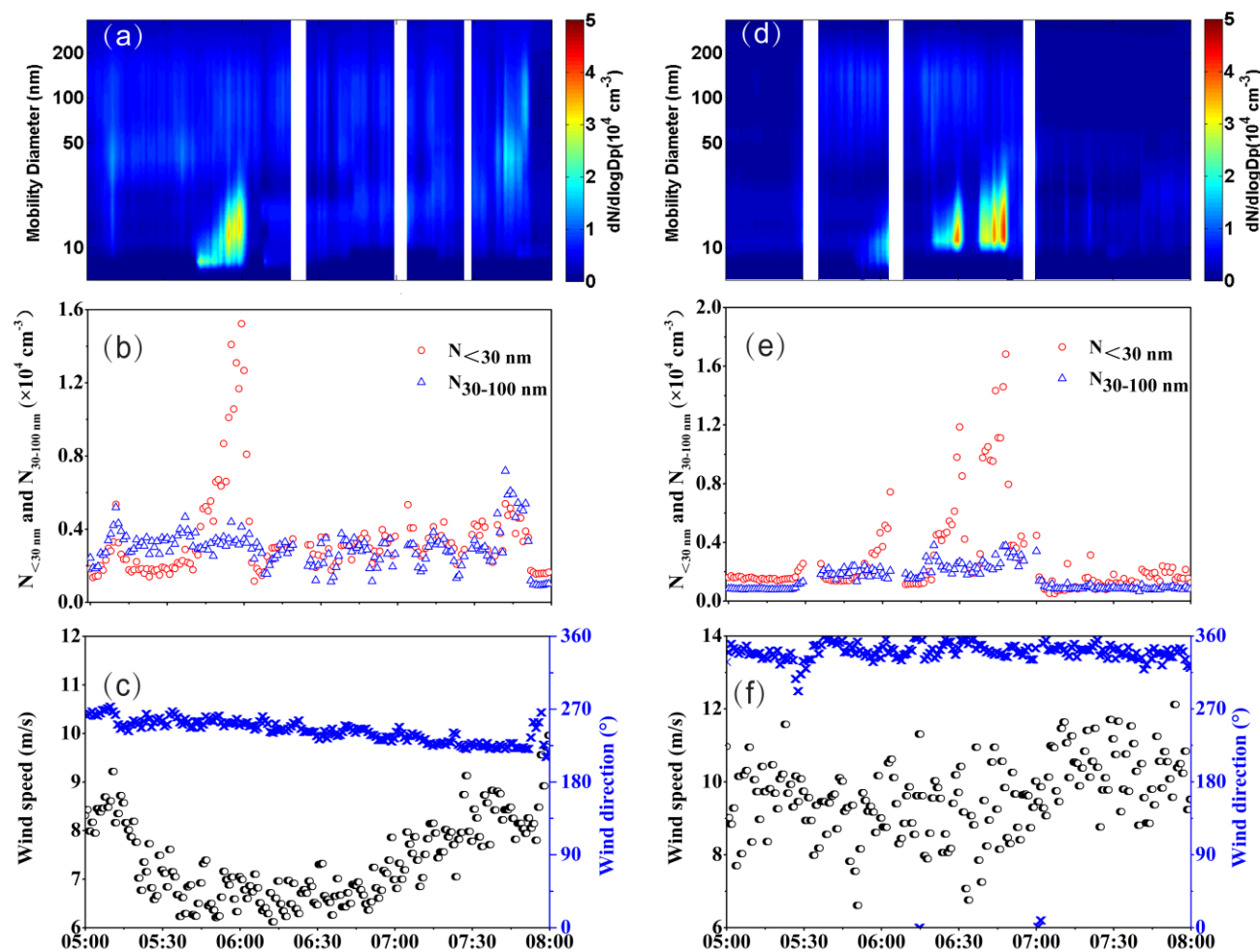
Figure 5 Temporal variations of particle number size concentrations, particle concentrations, and meteorological parameters for NPF events observed on DOY 98 (a, b, c) and DOY 103 (d, e, f) 2014. Data points suffering from ship self-emissions were removed to avoid clustering.
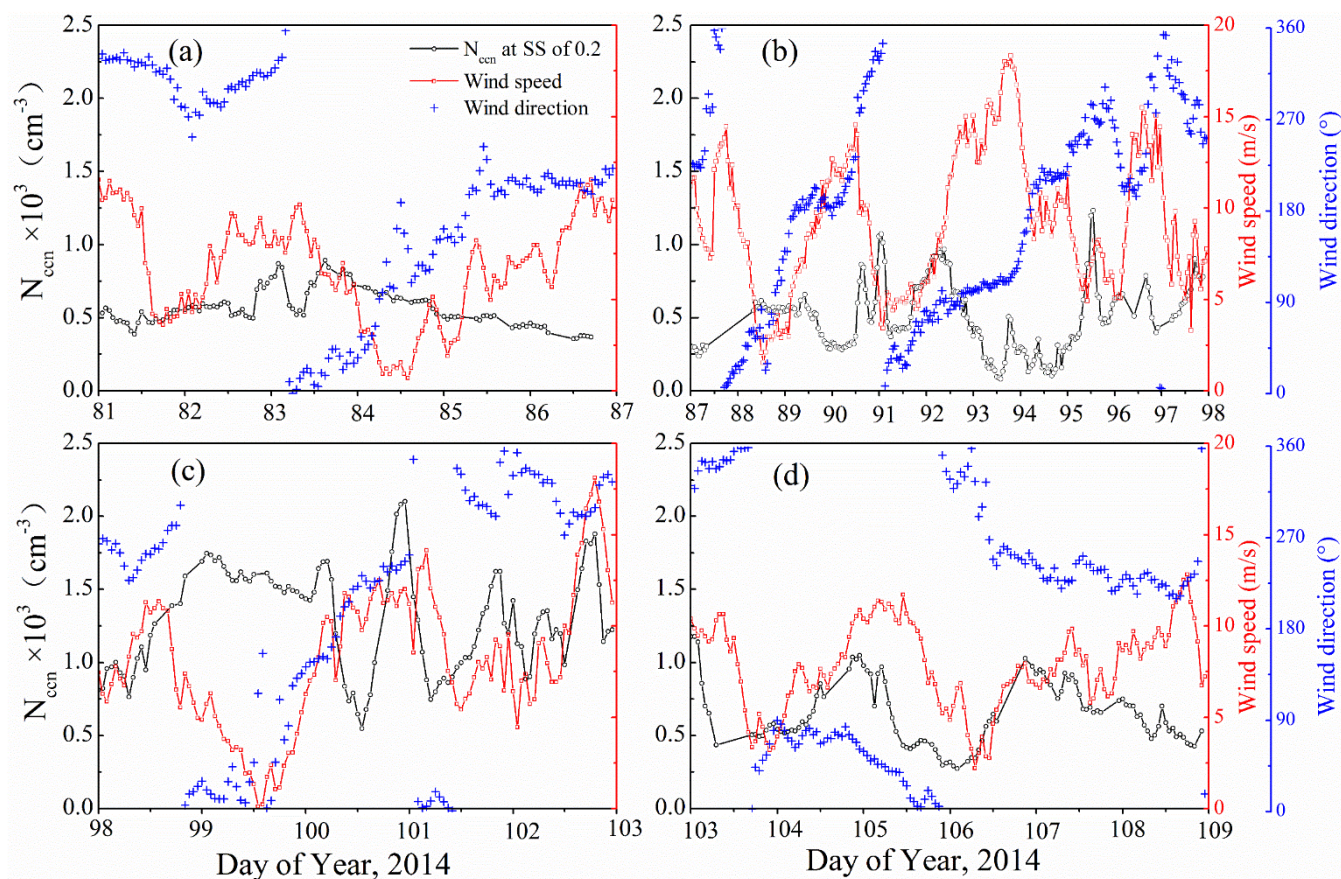
Figure 6 Time series of the N_{ccn}, wind speed and wind direction at SS of 0.2% during the measurement for the four periods, including Period 1 (a), Period 2 (b), Period 3 (c) and Period 4 (d).
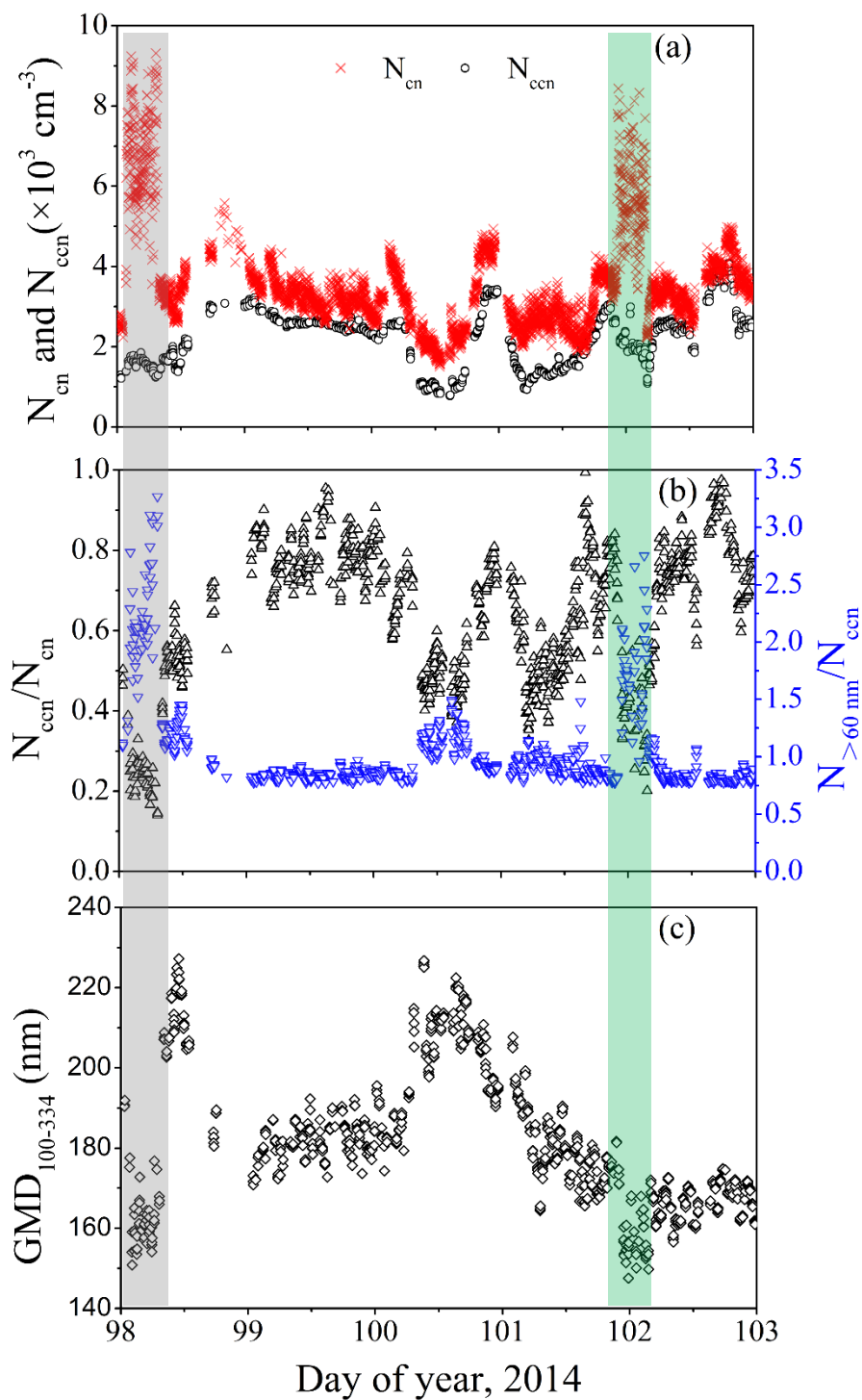
Figure 7 Time series of the N_{cn}, the bulk N_{ccn}, N_{ccn}/N_{cn}, $N_{>60\ nm}/N_{ccn}$ and GMD $_{100\text{-}334}$ at SS of 0.4% during DOY 98-102, 2014. The gray shading indicates the dust event and the green shading indicates the BB event.

Table 1 Concentrations of CN and CCN, AR, mixing ratios of O_3 and metrological conditions during DOY 81-108, 2014 over the NWPO.

Sampling periods	DOY 81-86 (Period 1)	DOY 87-97 (Period 2)	DOY 98-102 (Period 3)	DOY 103-108 (Period 4)	DOY 81-108
CN $(\times10^3)$ [a]	1.4-4.9, 2.8±0.51 [b]	1.7-5.0, 3.1±0.61*	1.5-9.3, 3.5±1.2	0.88-3.8, 2.0±0.53	0.88-9.3, 2.8±1.0
CCN$(\times10^3)$, SS=0.2%	0.34-0.94	0.07-1.4	0.53-2.2	0.25-1.3	0.07-2.2
	0.56±0.12	0.50±0.24	1.3±0.36	0.64±0.21	0.68±0.38
CCN$(\times10^3)$, SS=0.4%	0.47-1.6	0.12-2.3	0.77-4.1	0.33-2.6	0.12-4.1
	0.84±0.20	0.79±0.38	2.2±0.72	1.0±0.41	1.1±0.67
AR, 0.2%SS	0.09-0.38	0.11-0.42	0.09-0.65	0.13-0.59	0.08-0.65
	0.21±0.06	0.21±0.06*	0.38±0.11	0.32±0.08	0.30±0.11
AR, 0.4%SS	0.13-0.69	0.11-0.52	0.14-0.99	0.17-0.96	0.11-0.99
	0.32±0.09	0.30±0.08*	0.64±0.18	0.49±0.13	0.46±0.19
O_3 (ppb)	7-73, 52±12	0-68, 37±17	12-74, 55±12	27-67, 49±9	0-74, 47±14
RH (%)	43-95, 62±13	56-100, 83±13	39-94, 66±15	45-98, 66±14	39-100, 70±15
T (°C)	13.2-20.5, 17.3±1.8	12.1-21.7, 18.2±1.7	10.5-19.6, 16.0±2.1	8.6-20.3, 15.9±3.3	8.6-22.5,17.1±2.8
WS (m s^{-1})	0.9-11.6, 6.7±2.8	3.5-18.3, 10.1±4.1	0.8-18.3, 8.3±3.7	2.5-13.3, 7.9±2.3	0.8-18.3, 8.3±3.5

[a] Unit in $\times 10^3 cm^{-3}$

[b] Range and mean ± standard deviation

5   * The mean value during the measurement on DOY 96-97